

The homogeneous nucleation of 1-pentanol in a laminar flow diffusion chamber: The effect of pressure and kind of carrier gas

D. Brus,^{1,2,a)} A.-P. Hyvärinen,¹ J. Wedekind,³ Y. Viisanen,¹ M. Kulmala,⁴ V. Ždímal,² J. Smolík,² and H. Lihavainen¹

¹Finnish Meteorological Institute, Erik Palménin aukio 1, P.O. Box 503, FI-00101 Helsinki, Finland

²Laboratory of Aerosol Chemistry and Physics, Institute of Chemical Process Fundamentals, Academy of Sciences of the Czech Republic, Rozvojová 135, CZ-16502 Prague 6, Czech Republic

³Departament de Física Fonamental, Universtat de Barcelona, Martí i Franquès 1, ES-8028 Barcelona, Spain

⁴Department of Physical Sciences, University of Helsinki, P.O. Box 64, FI-00014 Helsinki, Finland

(Received 13 August 2007; accepted 29 February 2008; published online 7 April 2008)

The influence of total pressure and kind of carrier gas on homogeneous nucleation rates of 1-pentanol was investigated using experimental method of laminar flow diffusion chamber in this study. Two different carrier gases (helium and argon) were used in the total pressure range from 50 to 400 kPa. Nucleation temperatures ranged from 265 to 290 K for 1-pentanol-helium and from 265 to 285 K for 1-pentanol-argon. Nucleation rates varied between 10^1 and 10^6 $\text{cm}^{-3} \text{s}^{-1}$ for 1-pentanol-helium and between 10^2 and 10^5 $\text{cm}^{-3} \text{s}^{-1}$ for 1-pentanol-argon. Both positive and slight negative pressure effects were observed depending on temperature and carrier gas. The trend of pressure effect was found similar for both carrier gases. Error analysis on thermodynamic properties was conducted, and the lowering of surface tension due to adsorption of argon on nucleated droplets was estimated. A quantitative overview of pressure effect is provided. © 2008 American Institute of Physics. [DOI: 10.1063/1.2901049]

INTRODUCTION

Despite sedulous theoretical and experimental investigation of the influence of total pressure on homogeneous nucleation, this issue remains still unclear and open. Current paper presents another subsequent experimental work discussing pressure effect in a diffusion based device, laminar flow diffusion chamber (LFDC). An extensive review of carrier gas effect was done previously elsewhere.^{1,2} Only the latest theoretical investigations are mentioned here, and experiments made only in diffusion based devices are resumed.

The latest theoretical studies show quite surprising agreement in carrier gas pressure effect on nucleation. Barret³ using Metropolis Monte Carlo method predicted a significant increase in nucleation rate with increasing background gas pressure. The same results but with much higher magnitude were obtained by Merikanto *et al.*⁴ using novel Monte Carlo approach. Last two differ mainly in the way how the size of perturbation from equilibrium is estimated.³ Tang and Ford⁵ performed molecular dynamics simulations with isolated and thermostated Lennard-Jones argon clusters. They found a nonlinear stabilizing effect on clusters, being strongest at intermediate gas pressures. Yasuoka *et al.*⁶ using molecular dynamics simulations observed an increase of nucleation rate with increasing pressure or no effect depending on model used.

Considering systematic experimental research on pressure effect in alcohols and measurements conducted in diffusion based devices, some investigations have been already

done earlier by several research groups. In 1987 Chukanov and Kuligin⁷ measured dependence of critical supersaturation of water on total pressure and temperature.

In 1988 Katz *et al.*⁸ reported pressure effect in *n*-nonane using helium as a carrier gas. Between 1994 and 1998 Heist *et al.*⁹⁻¹² measured dependence of critical supersaturation on total pressure in several alcohols using high pressure thermal diffusion chamber. These measurements cover wide pressure range from 0.1 to 4 MPa. In 1995 Ždímal *et al.*¹³ measured critical supersaturation as a function of temperature in 1-propanol-helium at three levels of pressure: 50, 120, and 180 kPa. In 2006 Brus *et al.*¹ introduced a method where dependence of nucleation rate on total pressure was measured at constant temperature and supersaturation. Investigation was made in 1-propanol-helium at three levels of pressure: 50, 100, and 200 kPa and two isotherms of 280 and 290 K using a thermal diffusion cloud chamber (TDCC). All groups observed a decrease of nucleation rate with increasing pressure.

In 1995 Anisimov *et al.*¹⁴ used a LFDC to measure nucleation rates of 1-pentanol-helium as a function of supersaturation at three levels of total pressure: 0.1, 0.2, and 0.3 MPa and temperatures between 258 and 266 K. In 2006 Hyvärinen *et al.*^{2,15} used same method as Brus *et al.*¹ but in the LFDC. Nucleation rates of 1-butanol-helium were measured at three levels of pressure: 50, 100, and 210 kPa and temperatures ranging from 265 to 280 K. Anisimov *et al.*¹⁴ observed an increase of nucleation rate with increasing pressure, results of Hyvärinen *et al.*¹⁵ show the same trend, the increase of nucleation rate with increasing pressure, but with lower magnitude.

^{a)}Electronic mail: brus@icpf.cas.cz.

TABLE I. Thermodynamic properties of argon and the mixture of 1-pentanol-argon. M : Molar mass; κ : Thermal conductivity; C_p : heat capacity; η : Viscosity; D_{ab} : Binary diffusion coefficient; $1/\alpha$: Thermal diffusion factor; T : Temperature (K); P : Total pressure (Pa); y : Molar fraction of vapor.

Property	Equation	Unit	Reference
M	39.948	g mol^{-1}	
κ	$1 \times 10^{-4}(174.45 + 0.465(T - 293.15))$	$\text{W m}^{-1} \text{K}^{-1}$	18
C_p	520.677	$\text{J kg}^{-1} \text{K}^{-1}$	19
η	$1.95655 \times 10^{-5}(T^{1.5})/(T + 141.59)$	N s m^{-2}	20
D_{ab}	$1 \times 10^{-4}(0.00143T^{1.75}/((P/100000)54.98^{0.5}(113.33^{0.333} + 16.2^{0.333})^2))$	$\text{m}^2 \text{s}^{-1}$	19
$1/\alpha$	$((117.41/6.0365 + T/(6.0365(-95.773 + 0.43556T)))(y + 6.0365) - 117.41)$	1	21

In this work, we will present the measured nucleation rates of 1-pentanol as a function of total pressure ranging from 50 to 400 kPa with helium and argon as carrier gases. A comprehensive error analysis will be conducted, and critical cluster sizes will be determined. Results will be compared to theoretical predictions, as well as to earlier measurements made with the method presented by Brus *et al.*¹

EXPERIMENTAL METHOD

The nucleation measurements were performed in a LFDC first introduced in the work of Lihavainen and Viisanen.¹⁶ The necessary modifications of the LFDC for pressure investigation, principle of operation, data analysis, and verification of proper operation were already discussed in details in the previous paper,² so they will not be repeated here. Helium (Praxair, purity 99.9999%) and argon (AGA, purity 99.9999%) were used as carrier gases and 1-pentanol (Fluka, purity >99.0%) as the nucleating substance.

Proper flow rates were chosen according to conditions discussed previously,² for 1-pentanol-helium it was $900 \text{ cm}^3 \text{ min}^{-1}$ and for system 1-pentanol-argon $300 \text{ cm}^3 \text{ min}^{-1}$. These flow rates were measured with a bubble flow rate calibrator (Gilibrator 2, Sensidyne Inc., USA) at atmospheric pressure. The same flow rate was used for all levels of pressures. The flow rates were then converted to the pressure used in the LFDC with ideal gas law.

The thermodynamic properties of 1-pentanol, helium, and their mixtures are taken from Hyvärinen *et al.*¹⁷ The thermodynamic properties of argon and its mixture properties with 1-pentanol are listed in Table I. The same thermodynamic parameters and their estimations (e.g., Fuller method for binary diffusion coefficient) were and will be used for all measurements. This ensures a systematic use of the model calculations with different substances.

The experimental data for measurements on 1-pentanol in helium and 1-pentanol in argon is available online.²²

RESULTS AND DISCUSSION

Effect of total pressure

1-pentanol-helium

The isothermal nucleation rates of 1-pentanol in helium were measured between 10^1 and $10^6 \text{ cm}^{-3} \text{ s}^{-1}$ at nucleation

temperatures between 265 and 290 K in steps of 5 K. The isotherms at 265, 270, and 275 K were measured at pressures of 50, 100, 200, and 400 kPa, the isotherms at 280, 285, and 290 K were measured at pressures of 50, 100, and 200 kPa. The lower temperature limit was determined by the evaporation of droplets in the optical cell and the higher temperature limit by the released latent heat of condensation and depletion of vapor. The lower pressure limit was determined by safe operation of the optical cell and by keeping the nucleation zone far enough from the entrance of the condenser as discussed elsewhere.² The upper pressure limit was determined by stable operation of the LFDC. The measured particle concentration had the same limits, as reported in previous paper.²³

The isothermal nucleation rates as a function of saturation ratio at various pressure levels are illustrated in Fig. 1. The positive pressure effects can be seen in this figure; at all nucleation temperatures nucleation rate increases with increasing pressure. The isotherms measured at 50 kPa occur at higher saturation ratios than those ones measured at 100, 200, and 400 kPa. The different slopes of measured iso-

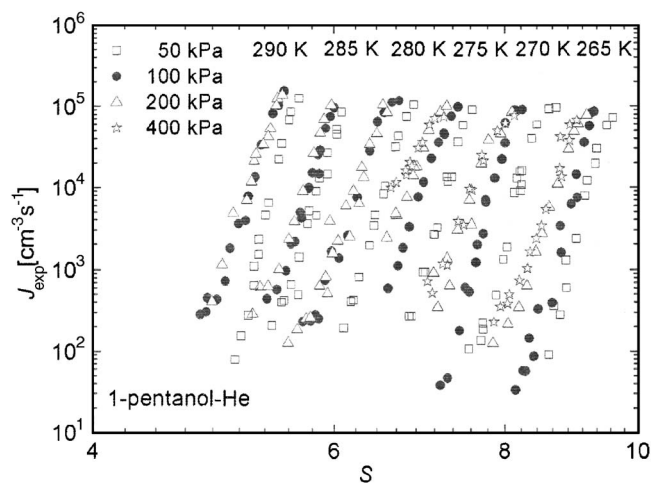


FIG. 1. The experimental nucleation rates J_{exp} as a function of saturation ratio S of 1-pentanol-helium system. Open squares are experimental data at 50 kPa, solid circles are data at 100 kPa, open triangles are data at 200 kPa, and open stars are data at 400 kPa. Isotherms from the right: 265, 270, 275, 280, 285, and 290 K.

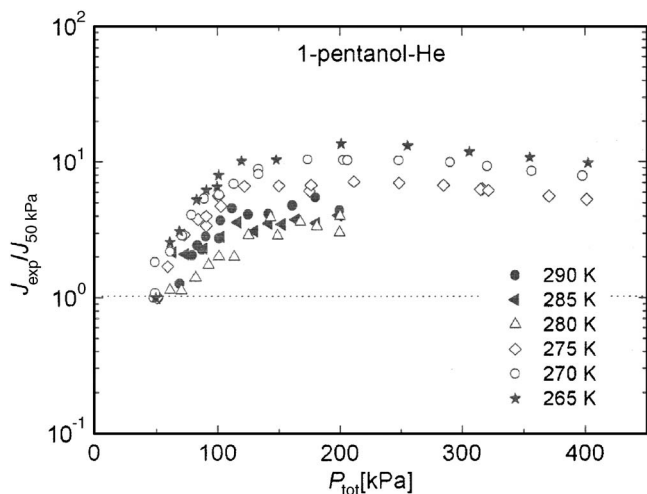


FIG. 2. Normalized experimental nucleation rates $J_{\text{exp}}/J_{50 \text{ kPa}}$ as a function of total pressure of 1-pentanol-helium. Solid stars are experimental data at 265 K, open circles are data at 270 K, open diamonds are data at 275 K, open triangles are data at 280 K, solid triangles are data at 285 K, and solid circles are data at 290 K.

therms at different pressures were observed. This observation was also made in previous paper, with increasing pressure the slope of isotherms decreases.^{2,15}

The dependence of normalized homogeneous nucleation rates $J_{\text{exp}}/J_{50 \text{ kPa}}$ on total pressure measured at nearly constant saturation ratio (± 0.03) for each isotherm can be seen in Fig. 2. The constant saturation ratio was chosen at experimental point of each isotherm in the place where all pressures can be covered. The normalization was done in a way that experimental point at the lowest pressure (~ 50 kPa) of each isotherm was set to 10^0 , and with increasing pressure, we could observe the trend and magnitude of the pressure effect. All isotherms show positive pressure effect from 50 to 200 kPa with a maximum magnitude of one order at 265 K. In the range from 200 to 400 kPa the dependence flattens.

1-pentanol-argon

The isothermal nucleation rates of 1-pentanol in argon were measured between 10^2 and $10^5 \text{ cm}^{-3} \text{ s}^{-1}$ at nucleation temperatures of 265, 270, 275, 280, and 285 K. The isotherms at 265 and 270 K were measured at pressures of 50, 100, 200, and 400 kPa, the isotherms at 275 and 280 K were measured at pressures of 50, 100, and 200 kPa, and the isotherm at 285 K was measured only at two pressures of 50 and 100 kPa. The lower and upper limits of the temperature and pressure are same as for 1-pentanol-helium system, both were discussed above.

The experimental nucleation rate measurement data of 1-pentanol-argon can be seen in Fig. 3. The pressure effect is very similar to that observed with 1-pentanol-helium: A slight negative or no effect at temperatures from 275 to 285 K, but a clear positive effect at nucleation temperatures of 270 and 265 K. The same difference in slopes was also observed as in system 1-pentanol-helium.

The dependence of normalized homogeneous nucleation rates $J_{\text{exp}}/J_{50 \text{ kPa}}$ on total pressure measured at nearly con-

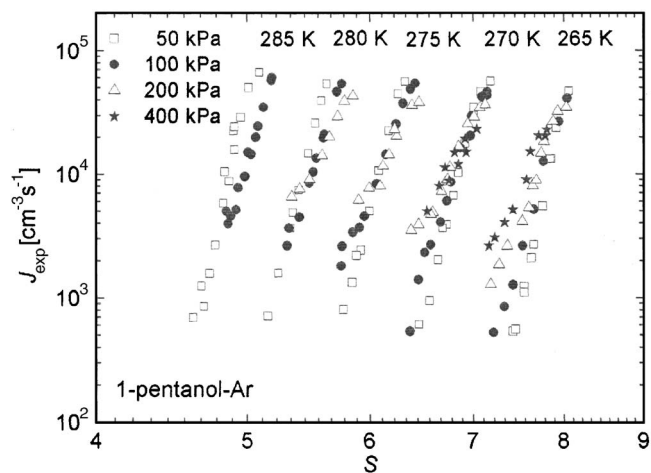


FIG. 3. The experimental nucleation rates J_{exp} as a function of saturation ratio S of 1-pentanol-argon system. Open squares are experimental data at 50 kPa, solid circles are data at 100 kPa, open triangles are data at 200 kPa, and solid stars are data at 400 kPa. Isotherms from the right: 265, 270, 275, 280, and 285 K.

stant saturation ratio (± 0.03) for each isotherm can be seen in Fig. 4. The constant saturation ratio was chosen in the same way as for system 1-pentanol-helium. The same holds for normalization. The isotherm at 280 K shows slight negative effect with about factor of 4, while the isotherm at 275 K shows no effect. Isotherms at 265 and 270 K show positive pressure effect with a maximum of one order in magnitude at 265 K. In the range from 200 to 400 kPa the dependence still increases unlike with helium as the carrier gas. This is denoted to the adsorption of argon on droplet surface, and is discussed in the following section.

Adsorption of carrier gas on droplet surface

The adsorption of gases on liquids may lower the surface tension of the liquid.²⁴ While helium typically causes no lowering to surface tension, the role of other low molecular

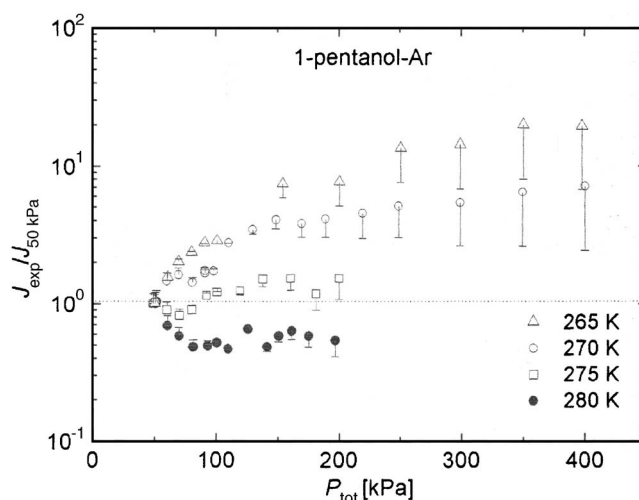


FIG. 4. Normalized experimental nucleation rates $J_{\text{exp}}/J_{50 \text{ kPa}}$ as a function of total pressure of 1-pentanol-argon system. Open triangles are experimental data at 265 K, open circles are data at 270 K, open squares are data at 275 K, and solid circles are data at 280 K. Error bars are estimations of nucleation rate without argon adsorption on droplet.

gases has been discussed in high pressure nucleation before.^{25–27} To estimate the effect of argon adsorption on nucleation, we have used the pressure dependent surface tension equation suggested by Luijten *et al.*,²⁵

$$\sigma(p) = \sigma(0) - n_0 k_B T \ln\left(\frac{p + p_L}{p_L}\right), \quad (1)$$

where $\sigma(0)$ is the surface tension of the liquid with respect to its own vapor, n_0 is the number of adsorption sites, approximately $6 \times 10^{18} \text{ m}^{-2}$, k_B is the Boltzmann constant, and p_L is the Langmuir pressure. We were unable to find pressure dependent surface tension data of 1-pentanol-argon. By using the knowledge that the change of surface tension is typically dependent on the adsorbing gas and not the liquid,²⁸ we have estimated the Langmuir pressure from a fit to $\sigma(p)$ data for water-argon system at room temperature,²⁴ obtaining value $p_L = 295.6$ bars. A constant Langmuir pressure can be applied for other temperatures, as observed by Luijten *et al.*²⁶ For obtaining $\sigma(0)$ from the measured surface tension data of 1-pentanol-air, $\sigma_{\text{pe-air}}$ at ambient pressure,²⁹ we have used

$$\sigma_{\text{pe}}(0) = \sigma_{\text{pe-air}} + n_0 k_B T \ln\left(\frac{1 \text{ bar} + p_{LN}}{p_{LN}}\right). \quad (2)$$

We have approximated the Langmuir pressure for air with the value of 326 bars used by Luijten *et al.*²⁵ for nitrogen. Equation (2) may also be used for estimating the surface tension of 1-pentanol against helium, which will differ slightly from the literature surface tension of 1-pentanol against air. Finally, we obtain for the pressure dependent surface tension for system 1-pentanol-argon

$$\sigma_{\text{pe-Ar}}(p) = \sigma_{\text{pe}}(0) - n_0 k_B T \ln\left(\frac{p + p_{LAr}}{p_{LAr}}\right). \quad (3)$$

While this equation is only qualitative due to the approximations made, it will give an estimation of the magnitude of the adsorption effect on nucleation rate. It should be noted that surface tension plays a negligible role while calculating the experimental nucleation rate through the mathematical fluid dynamics model in the LFDC. Only theoretical nucleation rate changes. The adsorption effect can be seen in Fig. 4. The error bars indicate the difference in nucleation rate calculated from the classical nucleation theory (CNT) with pressure independent surface tension and that obtained from Eq. (3). The calculation suggests that adsorption enhances the nucleation rate about half an order of magnitude at the maximum pressure of 400 kPa. This explains the increasing nucleation rate with pressure from 200 to 400 kPa. Without argon adsorption, a plateau similar to helium data would be observed, see Fig. 2.

Effect of the kind of carrier gas

The isothermal nucleation rates at 265 and 280 K measured in helium and argon at 200 kPa are presented in Fig. 5. The pressure was chosen so that there is a plateau in the pressure effect, and only the effect of carrier gas kind can be estimated. It can be seen that nucleation rates measured in argon shift to lower saturation ratios when compared to the

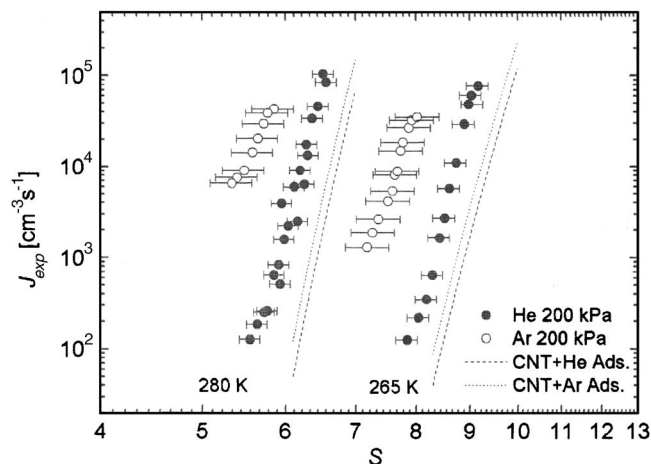


FIG. 5. The experimental nucleation rates J_{exp} as a function of saturation ratio S , the comparison between 1-pentanol-helium (solid circles) and 1-pentanol-argon (open circles) at pressure 200 kPa and two temperatures of 265 and 285 K. Data of 1-pentanol-argon at same temperature are shifted to lower saturation ratios from data of 1-pentanol-helium. Error bars are from the inaccuracy of the binary diffusion coefficient. Lines are predictions from CNT calculated with surface tensions from Eq. (2) for 1-pentanol-helium and Eq. (3) for 1-pentanol-argon.

helium results. Similar behavior has been repeatedly observed in laminar flow diffusion chambers.^{16,30} The difference is larger at 265 K.

There is some evidence pointing out that the uncertainties in transport properties may be the cause for the observed carrier gas kind effect in diffusion based devices. First of all, the carrier gas kind has not been observed to affect the nucleation rates measured in expansion devices,³¹ which are supposed to be independent of transport properties. Also, using more sophisticated fluid dynamics model (FLUENT-FPM) for LFDC with the same transport properties did not remove the effect, in fact, further increased it.³²

The thermodynamic properties most affecting the saturation ratio and temperature profiles in the tube flow are equilibrium vapor pressure, binary diffusion coefficient, and thermal conductivity of the mixture. Equilibrium vapor pressure does not depend on the carrier gas. Thermal conductivity is mostly governed by the carrier gas. However, thermal conductivity of both helium and argon are known with a sufficient accuracy. In this inspection we will only focus on diffusion coefficient.

As was done in the previous paper,² we estimate the uncertainty for the property and apply the perturbed value in the mathematical model for calculation of new nucleation temperature and saturation ratio. The error for binary diffusion coefficient from the Fuller method¹⁹ was estimated to be 5% both for 1-pentanol-helium and 1-pentanol-argon mixtures. It is important to point out here that the Fuller method may overestimate the diffusion coefficient for one liquid-gas mixture, but underestimate it for the same liquid but different gas mixture. This is the case, for example, with benzene-helium and benzene-argon mixtures.¹⁹

The calculation was performed at pressure of 200 kPa for both carrier gas-liquid mixtures at 265 and 280 K. Results are illustrated in Fig. 5. At 265 K, the effect on saturation ratios are ± 0.36 for argon as carrier gas and ± 0.20 with

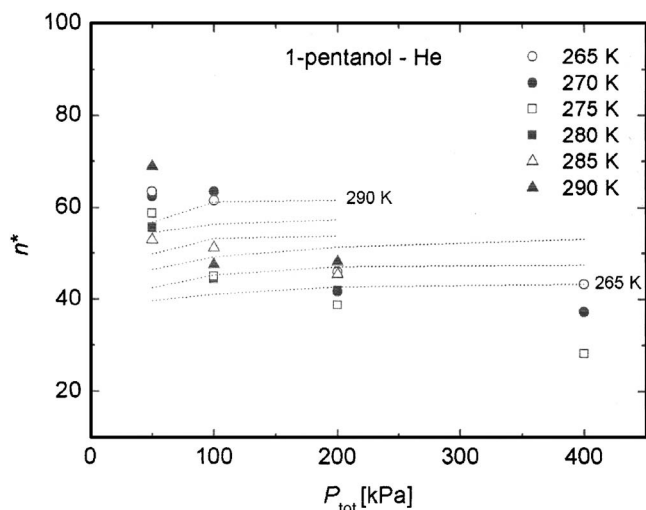


FIG. 6. Critical cluster sizes n^* of 1-pentanol-helium as a function of total pressure P_{tot} . Points are values calculated with nucleation theorem and dotted lines are predictions of Kelvin equation calculated with critical saturation ratios at nucleation rate of $10^4 \text{ cm}^{-3} \text{ s}^{-1}$ for temperatures from 265 to 290 K with a step of 5 K.

helium as carrier gas. At 280 K the effects are ± 0.25 for argon as carrier gas and ± 0.14 with helium as carrier gas. Nucleation temperatures are less affected, the average is about 0.15 K for both carrier gases.

Also the adsorption effect of carrier gas on droplet is estimated in Fig. 5. Nucleation rate from CNT was calculated from Eq. (2) with helium adsorption and from Eq. (3) with argon adsorption taken into account. With these new surface tension values it can be seen that a slight difference in nucleation rates is expected when carrier gas is changed. Uncertainties in diffusion coefficient combined with the change of nucleation rate due to adsorption of carrier gas on droplet are just about able to explain the carrier gas kind effect at 280 K, but not quite at 265 K.

Critical cluster sizes

The sizes of critical clusters were calculated from the first nucleation theorem,³³

$$\left(\frac{\partial \ln J}{\partial \ln S} \right)_T = n^*. \quad (4)$$

The critical cluster sizes for 1-pentanol-helium and 1-pentanol-argon determined as a function of pressure are illustrated in Figs. 6 and 7, respectively. It can be seen that according to these measurements, critical cluster size depends on total pressure. According to our measurements critical clusters are almost twice as big at 50 kPa as at 400 kPa, however, for 1-pentanol-helium at lower pressures the scatter in data is large. There is also slight inconsistency of critical cluster sizes at low temperature isotherms at 270 and 265 K because of evaporation of droplets in optical cell.²³ The error due to evaporation is more pronounced at low nucleation rates, making the slope of the isotherms steeper. If the slope of 270 K isotherm is calculated from nucleation rates higher than $10^4 \text{ cm}^{-3} \text{ s}^{-1}$, the critical cluster size of ~ 50 molecules is obtained. At 265 K the vapor pres-

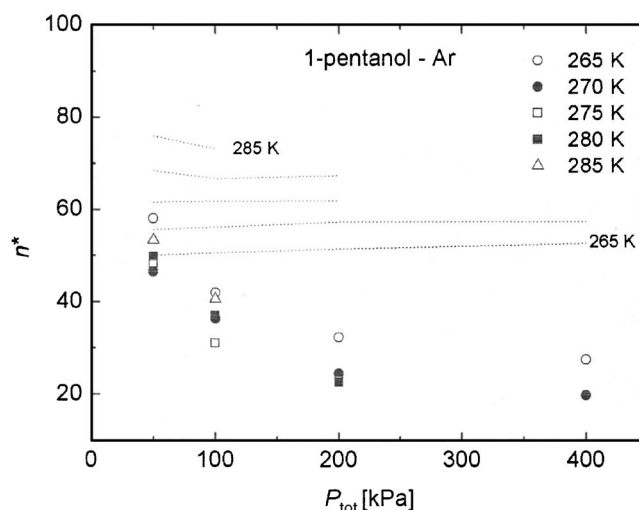


FIG. 7. Critical cluster sizes n^* of 1-pentanol-argon as a function of total pressure P_{tot} . Points are values calculated with nucleation theorem, and dotted lines are predictions of Kelvin equation calculated with critical saturation ratios at nucleation rate of $10^4 \text{ cm}^{-3} \text{ s}^{-1}$ for temperatures from 265 to 285 K with a step of 5 K.

sure of 1-pentanol is so low that together with the evaporation effect, the experimental limit is too close for an accurate determination of n^* . In general, critical cluster sizes predicted by the Kelvin equation agree quite well with nucleation theorem to pretty small sizes, but this is not valid for our 1-pentanol-argon measurements (see dotted line in Fig. 7). Critical cluster sizes determined from the argon measurements are considerably smaller than those measured in helium (Figs. 6 and 7).

Comparison against theory

The measured nucleation rates were compared against the CNT (Ref. 34) and the extended modified liquid drop model nucleation theory (EMLDM-DNT).^{35,36} Pressure independent surface tensions were used for calculating the theoretical values. The nucleation rates normalized to theoretical ones are presented in Fig. 8. It can be seen that nucleation rates measured in helium are, in general, closer to theoretical predictions, and nucleation rates measured in argon are always higher than predicted by both CNT and EMLDM-DNT theories. The temperature dependence changes with total pressure. At 200 kPa, both CNT and EMLDM-DNT predict temperature dependence close to the experimental results. At this pressure, the nucleation rates predicted by EMLDM-DNT are within one order of magnitude of the experimental ones measured in helium. The 400 kPa measurements do not cover the whole temperature range, which might distort the temperature dependence compared to other temperatures.

OVERVIEW OF PRESSURE EFFECT

In this section we would like to provide a short quantitative overview of our recent work on pressure effect in diffusion chambers. It is illustrated in Figs. 9 and 10, where the results of three already measured substances are shown. The experimental results of 1-pentanol-helium and 1-pentanol-argon obtained in this study; 1-propanol-helium at 290 K

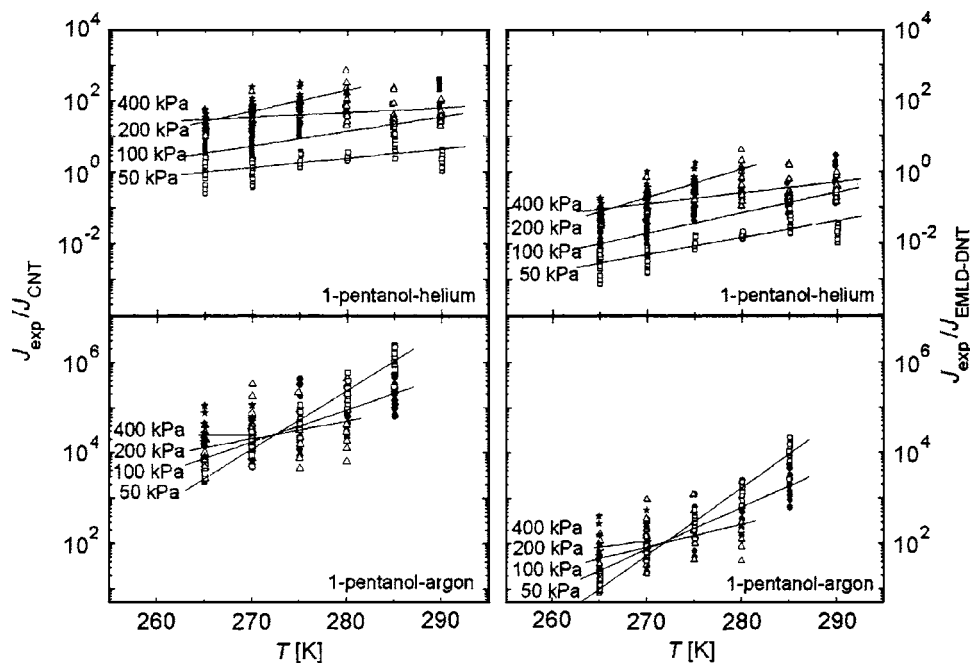


FIG. 8. The ratio of experimental and theoretical nucleation rates $J_{\text{exp}}/J_{\text{the}}$ as a function of temperature T . Left hand side: CNT used as theory. Right hand side: EMLDM-DNT used as theory. Upper figures: Carrier gas helium. Lower figures: Carrier gas argon. Lines are linear fits to data at different pressures.

with two different saturation ratios and 1-butanol-helium at 290 K measured in TDCC;^{1,23} and finally 1-butanol-helium measured in LFDC.¹⁵ The orders of magnitudes of the pressure effect at the pressure range of these measurements are plotted as a function of temperature and saturation ratio, Figs. 9 and 10, respectively. These figures are made with the help of Figs. 2 and 4, but only last point in a “plateau region” of each measured isotherm is taken in to account, e.g., the last point at temperature of 265 K and pressure of 400 kPa in Fig. 2 provides positive pressure effect of one order of magnitude. This point corresponds to the leftmost upper open circle in Fig. 9 and rightmost upper open circle in Fig. 10. All other points for all above mentioned systems are processed in the same way.

In addition we can see from Fig. 9 that lighter vapor

(1-butanol in LFDC) at higher temperature (e.g., 280 K) shows weaker positive pressure effect than heavier vapor (1-pentanol in LFDC) at the same temperature. The same trend holds for 1-propanol and 1-butanol in TDCC. Similar conclusions might be drawn from Fig. 10, where the pressure effect shows a clear relation to the saturation ratio, regardless of substance.

It can be seen that the pressure effect is systematic both in LFDC and TDCC when measured with three different substances, and according to Fig. 10, the pressure effect may even be predicted to some extent. For 1-hexanol, for example, the measurements in LFDC working conditions are typically conducted in saturation ratios ranging from 6 to 14, so we would expect to see slight negative (if any) or only positive pressure effect.

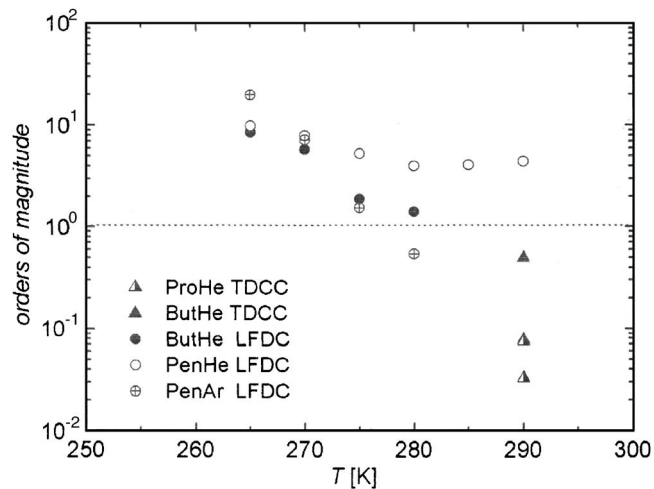


FIG. 9. The pressure effect in orders of magnitude as a function of temperature T . Triangles are data from TDCC, half-filled triangles are data of 1-propanol-helium, and solid triangles are data of 1-butanol-helium. Circles are data from LFDC, solid circles are data of 1-butanol-helium, open circles are data of 1-pentanol-helium, and crossed circles are data of 1-pentanol-argon.

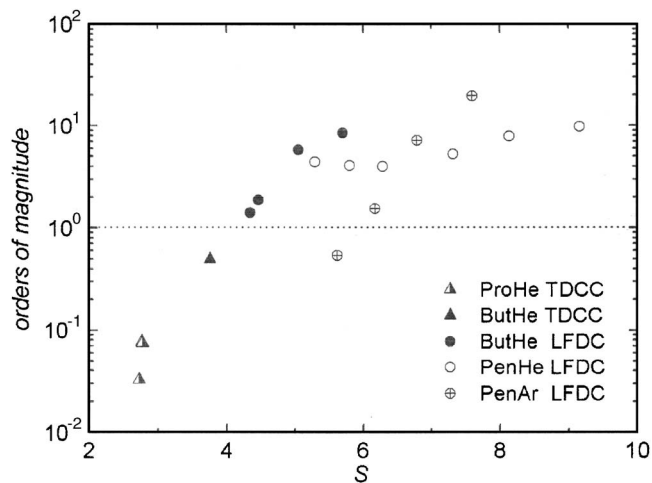


FIG. 10. The pressure effect in orders of magnitude as a function of saturation ratio S . Triangles are data from TDCC, half-filled triangles are data of 1-propanol-helium, and solid triangles are data of 1-butanol-helium. Circles are data from LFDC, solid circles are data of 1-butanol-helium, open circles are data of 1-pentanol-helium, and crossed circles are data of 1-pentanol-argon.

CONCLUSIONS

Nucleation rates of 1-pentanol were measured in a LFDC using helium and argon as carrier gases, at pressures from 50 to 400 kPa, and at temperatures from 265 to 290 K. Both negative and positive pressure effects were observed, depending on temperature and carrier gas. This suggests that there are at least two competing mechanisms affecting nucleation. The effect was similar both in helium and argon.

The carrier gas pressure effect was noticed only at lower pressures. At pressures higher than 200 kPa no pressure effect is observed, as long as the conditions of gas-vapor non-idealities are not entered. Both CNT and extended modified liquid drop model theory estimated nearly correct temperature dependence at 200 kPa.

Interestingly, the measurements also suggest that the critical cluster size depends on pressure, with highest cluster sizes occurring at lower pressures. Measurements in argon yield generally lower critical cluster sizes.

To consolidate the differences between nucleation rates measured in argon and helium, we took into account the inaccuracy of binary diffusion coefficient, the relatively most important parameter affecting the flow profile calculations with different carrier gases. It is also a parameter not needed in expansion chamber measurements, which do not yield a carrier gas kind effect. In addition, we took into account the change in surface tension due to adsorption of carrier gas on droplet. The adsorption effect was able to explain for the rising trend in pressure effect at higher pressure for argon. Uncertainties in diffusion coefficient combined with the change of nucleation rate due to adsorption of carrier gas on droplet might be able to explain the carrier gas kind effect at 280 K, but not quite at 265 K.

According to our studies, even though both positive and negative carrier gas pressure effects are observed in nucleation measurements, the results are systematic. The pressure effect shows clear relation to both nucleation temperature and saturation ratio regardless of substance in two different devices (LFDC and TDCC), suggesting that using a lighter vapor enhances the negative effect.

In this work, we have made further steps in understanding the mechanisms behind carrier gas pressure and kind effects in the LFDC. However, the evidence is still indicative rather than conclusive. We identify three methods for improving the knowledge of this problem. More measurements are needed to verify the relationship of vapor properties to the pressure effect. The accuracy of the mathematical model should be tested against a more sophisticated model with different vapors especially at lower pressures. Finally, accurate theoretical predictions of the magnitude of pressure effect should be conducted at thermodynamic conditions similar to those used in the experiments.

ACKNOWLEDGMENTS

This work was supported by the Nordic Center of Excellence BACCI, Academy of Finland and Czech Science Foundation Grant No. 101/05/2214. The authors would like to acknowledge Joonas Vanhanen for help with extensive measurements during his nucleation course in Finnish Meteorological Institute in spring 2007.

- ¹D. Brus, V. Ždímal, and F. Stratmann, *J. Chem. Phys.* **124**, 164306 (2006).
- ²A.-P. Hyvärinen, D. Brus, V. Ždímal, J. Smolík, M. Kulmala, Y. Viisanen, and H. Lihavainen, *J. Chem. Phys.* **124**, 224304 (2006).
- ³J. C. Barrett, *J. Chem. Phys.* **126**, 074312 (2007).
- ⁴J. Merikanto, E. Zapadinsky, and H. Vehkamäki, *J. Chem. Phys.* **125**, 084503 (2006).
- ⁵H. Y. Tang and I. J. Ford, *J. Chem. Phys.* **125**, 144316 (2006).
- ⁶K. Yasuoka and X. C. Zeng, *J. Chem. Phys.* **126**, 124320 (2007).
- ⁷V. N. Chukanov and A. P. Kuligin, *Teplofiz. Vys. Temp.* **25**, 70 (1987).
- ⁸J. L. Katz, C.-H. Hung, and M. Krasnopoler, *Proceedings of the 12th ICNAA, Vienna* (Springer-Verlag, Berlin, 1988), p. 356.
- ⁹R. H. Heist, M. Janjua, and J. Ahmed, *J. Phys. Chem.* **98**, 4443 (1994).
- ¹⁰R. H. Heist, M. Janjua, and J. Ahmed, *J. Phys. Chem.* **99**, 375 (1995).
- ¹¹A. Bertelsmann, R. Stuczynski, and R. H. Heist, *J. Phys. Chem.* **100**, 23 (1996).
- ¹²A. Bertelsmann and R. H. Heist, *Aerosol Sci. Technol.* **28**, 3 (1998).
- ¹³V. Ždímal, J. Smolík, and H. Uchtmann, *J. Aerosol Sci.* **26**, 625 (1995).
- ¹⁴M. P. Anisimov, K. M. Anisimov, I. V. Gribanov, R. Y. Zamarayev, N. N. Nalimova, and Y. I. Povolnyaev, *Colloid J.* **56**, 407 (1994).
- ¹⁵A.-P. Hyvärinen, D. Brus, V. Ždímal, J. Smolík, M. Kulmala, Y. Viisanen, and H. Lihavainen, *J. Chem. Phys.* **128**, 109901 (2008).
- ¹⁶H. Lihavainen and Y. Viisanen, *J. Phys. Chem. B* **105**, 11619 (2001).
- ¹⁷A.-P. Hyvärinen, H. Lihavainen, Y. Viisanen, and M. Kulmala, *J. Chem. Phys.* **120**, 24 (2004).
- ¹⁸V. B. Mikheev, N. S. Laulainen, S. E. Barlow, M. Knott, and I. J. Ford, *J. Chem. Phys.* **113**, 9 (2000).
- ¹⁹R. C. Reid, J. M. Prausnitz, and B. E. Poling, *The Properties of Gases and Liquids*, 4th ed. (McGraw-Hill, New York, 1987).
- ²⁰R. H. Perry, D. W. Green, and J. O. Maloney, *Perry's Chemical Engineer's Handbook*, 6th ed. (McGraw-Hill, New York, 1983), pp. 3–248.
- ²¹J. Vašáková and J. Smolík, *Rep. Ser. Aerosol Sci.* **25**, 1 (1994).
- ²²See EPAPS Document No. E-JCPSA6-128-004815 for experimental data of nucleation of 1-pentanol in helium and argon. For more information on EPAPS, see <http://www.aip.org/pubservs/epaps.html>.
- ²³D. Brus, A.-P. Hyvärinen, V. Ždímal, and H. Lihavainen, *J. Chem. Phys.* **122**, 214506 (2005).
- ²⁴R. Massoudi and A. D. King Jr., *J. Phys. Chem.* **78**, 2282 (1974).
- ²⁵C. C. M. Luijten, K. J. Bosschaart, and M. E. H. van Dongen, *J. Chem. Phys.* **106**, 8116 (1997).
- ²⁶C. C. M. Luijten, P. Peeters, M. E. H. van Dongen, *J. Chem. Phys.* **111**, 8524 (1999).
- ²⁷C. C. M. Luijten and M. E. H. van Dongen, *J. Chem. Phys.* **111**, 8535 (1999).
- ²⁸R. Massoudi and A. D. King, *J. Phys. Chem.* **79**, 1676 (1975).
- ²⁹R. Strey and T. Schmeling, *Ber. Bunsenges. Phys. Chem.* **87**, 324 (1983).
- ³⁰K. Hämeri and M. Kulmala, *J. Chem. Phys.* **105**, 17 (1996).
- ³¹K. Iland, J. Wedekind, J. Wölk, P. E. Wagner, and R. Strey, *J. Chem. Phys.* **121**, 24 (2004).
- ³²E. Herrmann, H. Lihavainen, A.-P. Hyvärinen, I. Riipinen, M. Wilck, F. Stratmann, and M. Kulmala, *J. Phys. Chem. A* **110**, 12448 (2006).
- ³³D. Kashchiev, *J. Chem. Phys.* **104**, 8671 (1996).
- ³⁴R. Becker and W. Döring, *Ann. Phys.* **26**, 719 (1935).
- ³⁵D. Reguera and H. Reiss, *Phys. Rev. Lett.* **93**, 165701 (2004).
- ³⁶D. Reguera and H. Reiss, *J. Phys. Chem. B* **108**, 19831 (2004).